Mössbauer Study and Magnetic Properties of M-Type Barium Hexaferrite Doped with Co + Ti and Bi + Ti Ions

A. G. Belous,[†] O. I. V'yunov,*[,†] E. V. Pashkova,[†] V. P. Ivanitskii,[‡] and O. N. Gavrilenko[†]

V. I. Vernadskii Institute of General and Inorganic Chemistry, Kyiv 03680, Ukraine, and Institute of Geochemistry, Mineralogy and Ore Formation, Kyiv 03680, Ukraine

Received: July 21, 2006; In Final Form: September 21, 2006

Using X-ray powder diffractions, Mössbauer spectroscopy, and magnetic measurements, the effect of complex dopants (Co^{2+} + Ti^{4+}) and (Bi^{3+} + Ti^{4+}) on the fine structure and magnetic properties of M-type barium hexaferrite prepared by hydroxide and carbonate precipitations has been studied. The distribution of cations over five nonequivalent positions of barium hexaferrite with magnetoplumbite structure is discussed. It has been shown that doped barium hexaferrite can be used for high-coercitivity data storage media.

1. Introduction

M-type barium hexaferrite (BHF) with magnetoplumbite structure is widely used in devices for different purposes.[1,2] Hexagonal ferrites can be used in microwave devices working at high frequencies (above 100 GHz) due to their high uniaxial anisotropy and relatively small width of ferromagnetic resonance line.[3] Modified BHFs are of interest as promising high-coercitivity data storage media with high recoding density.[4−7]

To ensure the reliability of data carriers and their high performance, the value of coercitive force H_c must be large enough. However, there is a limitation for H_c due to difficulties of containment of strong magnetic field during recording on high-coercitivity filler and due to complication of recording device. It is known that substitution of Co^{2+} and Ti^{4+} ions for Fe^{3+} ions is used to decrease the coercitive force in BHF for magnetic recording.[8,9] Only synthesis from solutions can meet the stringent requirements to the fineness and morphology of the particles of these materials: high homogeneity, optimal size, and strong shape anisotropy. In recent years, the preparation of nanostructured BHF by sol−gel method has been increasing.[2,4−7] It is known that preparation of precursors by precipitation of slightly soluble compounds (hydroxides, carbonates) is simplest. However, the literature data relating to the effect of these precursors on the structure features and magnetic properties of BHF are very limited.[4−6] Preparation of materials with required characteristics requires the knowledge of dopant effect on the fine structure of BHF.

Cobalt is relatively expensive and has low handleability in the case when ammonium-containing precipitants are used. Therefore, the search for other dopants in decreasing coercive force is topical. Bismuth oxide suppresses grain growth during sintering in some ferrites,[10] and this impelled us to study also the effect of Bi^{3+} ions on coercive force in BHF with the aim to prepare ferromagnetic fillers for data carriers based on Bi^{3+}-doped BHF.

The aim of this work is the investigation of the effect of aliovalent substitution of (Co^{2+} + Ti^{4+}) and (Bi^{3+} + Ti^{4+}) ions for Fe^{3+} ions on the properties of BHF and distribution of cations over crystallographic positions.

2. Experimental Methods

Synthesis. Samples of the systems $BaCo_xTi_xFe_{12-2x}O_{19\pm\gamma}$ (**I**) and $BaBi_xTi_xFe_{12-2x}O_{19\pm\gamma}$ (**II**) were investigated. Hydroxide-carbonate precipitates were prepared by two-step precipitation of slightly soluble compounds of barium, cobalt(II), iron(III), bismuth(III), and titanium(IV). The preparation was performed at room temperature and at constant value of pH to ensure maximum precipitation. The pH of solution was adjusted using the automatic titration unit BAT-15. 1 M water solutions of ultrapure $BaCl_2$, $Co(NO_3)_2$, $Fe(NO_3)_3$, $Bi(NO_3)_3$, and $TiOCl_2$ were used.

For (Co^{2+} + Ti^{4+}) dopant (system I), hydroxides of Fe(III) and Ti(IV) were coprecipitated with a water solution of ammonia. Precipitates were washed in distilled water to remove NH^{4+} ions. Then cobalt(II) and barium carbonates were coprecipitated with a solution of sodium carbonate.

For (Bi^{3+} + Ti^{4+}) dopant (system II), hydroxides of Fe(III), Ti(IV), and Bi(III) were coprecipitated. Then barium carbonate was precipitated with ammonia carbonate as a precipitant.

Finally, the precipitates of both systems were washed free from the mother solution using distilled water until no NO_3^- and Cl^- ions in the washed solution were detected. Powders were dried at 390 K and heat-treated at 1270 K.

X-ray Powder Diffraction. X-ray powder diffraction (XRPD) patterns were obtained using a DRON-4-07 diffractometer (Cu Kα radiation).

Mössbauer Spectroscopy. The Mössbauer spectra (MS) were recorded at room temperature with a spectrometer working in the mode of constant accelerations with the use of ^{57}Co in Pd matrix. The speed scale was calibrated using α-Fe lines. MS were fitted using least-squares method.

Magnetic Measurements. Magnetic properties of powder samples were studied by means of a superconducting quantum interference device magnetometry (SQUID Quantum Design MPMS-5S, San Diego, CA). Hysteresis loops (demonstrating the main magnetic parameters of coercitive force, specific saturation magnetization, and maximal and residual magnetic induction[11]) were measured at room temperature in magnetic fields ranging from 0 to 15 kOe.

* To whom correspondence should be addressed. Telephone/fax: +380-44-4242211. E-mail: vyunov@ionc.kar.net.

[†] V. I. Vernadskii Institute of General and Inorganic Chemistry.

[‡] Institute of Geochemistry.

10.1021/jp064628t CCC: $33.50
Published on Web 12/02/2006

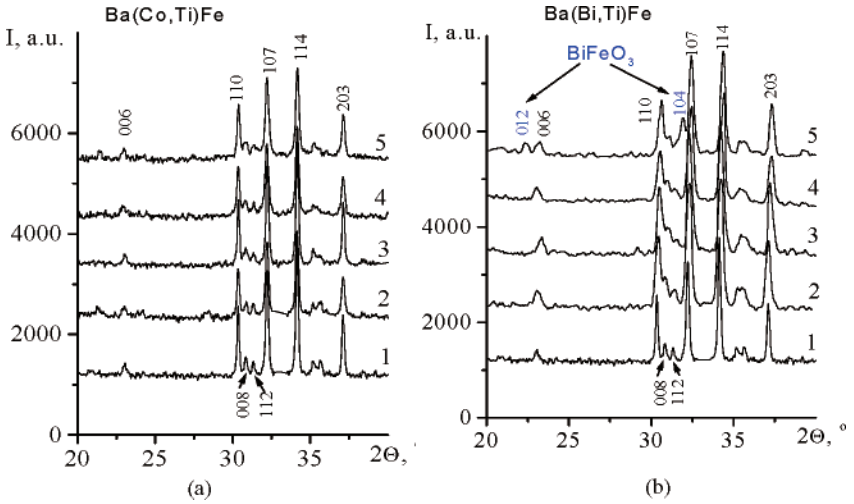

Figure 1. X-ray powder diffraction patterns of $BaCo_xTi_xFe_{12-2x}O_{19\pm\gamma}$ (a) and $BaBi_xTi_xFe_{12-2x}O_{19\pm\gamma}$ (b). (a) $x = 0$ (1), 0.1 (2), 0.15 (3), 0.45 (4), and 0. 8 (5); (b) $x = 0$ (1), 0.05 (2), 0.075 (3), 0.15 (4), and 0.2 (5).

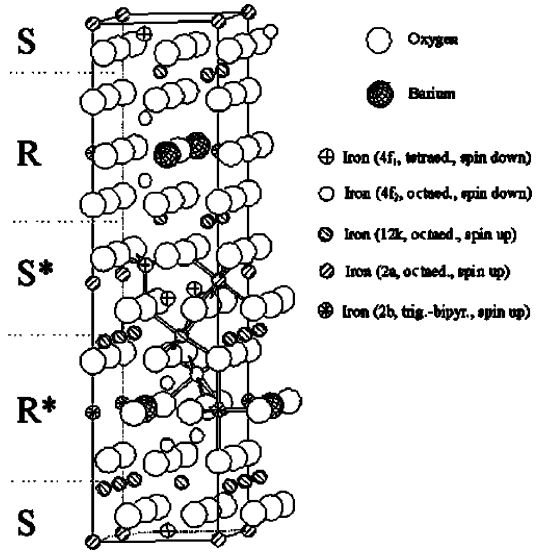

Figure 2. Structure of M-type barium hexaferrite or magnetoplumbite.[12]

3. Results and Discussion

X-ray Powder Diffraction. XRPD shows that $BaCo_xTi_xFe_{12-2x}O_{19\pm\gamma}$ ($x = 0-1$) (I) and $BaBi_xTi_xFe_{12-2x}O_{19\pm\gamma}$ ($x = 0-0.15$) (II) samples are single-phase and have a hexagonal M-type magnetoplumbite structure (space group $P6_3/mmc$). In system II, in addition to BHF phase, a rhombohedral $BiFeO_3$ phase also appears at $x = 0.2$ (Figure 1).

The structure of M-type BHF consists of spinel blocks *S*, *S** and hexagonal barium-containing blocks *R*, *R** alternating in the direction of the *c* axis. *S** and *R** blocks ensue on rotation of the *S* and *R* blocks by 180° about the *c* axis. The unit cell of BHF contains 10 layers of O^{2-} ions (Figure 2).[12] There are five nonequivalent crystallographic positions of iron ions in the structure; among them three are octahedral (12*k*, $4f_2$ and 2*a*), one is tetrahedral ($4f_1$), and the 2*b* position is an inside oxygen bipyramid.

Mössbauer Spectra. MS of samples I ($x = 0-0.8$) and II ($x = 0.15$) are shown in Figure 3, and their parameters are listed in Table 1. The MS lines were assigned to structural positions by the model described in refs 13−16, according to which each of the five positions of iron in the BHF structure produces a resonance sextet of magnetic interaction. The half-widths of the MS lines in every sextet were assumed to be identical. This model allows one to estimate the occupation of all structural positions by Fe^{3+} ions in single-phase BHF with well-crystallized structure.

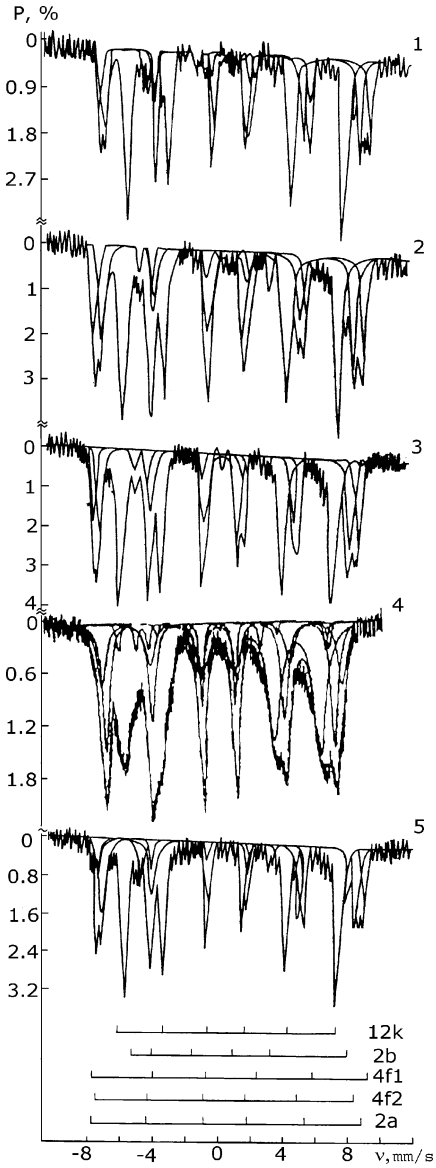

Figure 3. Mössbauer spectra of $BaCo_xTi_xFe_{12-2x}O_{19\pm\gamma}$ at $x = 0$ (1), 0.15 (2), 0.2 (3), and 0.8 (4) and $BaBi_xTi_xFe_{12-2x}O_{19\pm\gamma}$ at $x = 0.15$ (5).

TABLE 1: Parameters of Mössbauer Spectra of Doped Barium Hexaferrite[a]

		$BaCo_xTi_xFe_{12-2x}O_{19\pm\gamma}$				$BaBi_xTi_xFe_{12-2x}O_{19\pm\gamma}$
position	parameter	$x = 0$	$x = 0.15$	$x = 0.2$	$x = 0.8$	$x = 0.15$
	H_{eff}, kOe	419	417	418	403	420
12*k*	IS, mm/s	0.37	0.37	0.37	0.37	0.37
octahedron	QS, mm/s	0.42	0.40	0.40	0.28	0.41
	FWHM, mm/s	0.34	0.45	0.47	1.02	0.39
	S, %	48.9	50.6	51.4	50.1	50.8
	H_{eff}, kOe	497	491	490	474	496
$4f_1$	IS, mm/s	0.27	0.28	0.29	0.31	0.30
tetrahedron	QS, mm/s	0.23	0.20	0.19	0.13	0.17
	FWHM, mm/s	0.37	0.42	0.45	0.58	0.43
	S, %	23.3	21.3	24.7	27.6	24.9
	H_{eff}, kOe	525	519	520	499	522
$4f_2$	IS, mm/s	0.39	0.40	0.39	0.43	0.41
octahedron	*i*, mm/s	0.16	0.10	0.16	0.11	0.19
	FWHM, mm/s	0.28	0.35	0.25	0.72	0.28
	S, %	14.4	15.1	12.0	13.1	12.2
	H_{eff}, kOe	513	508	505	428	517
2*a*	IS, mm/s	0.38	0.37	0.39	0.37	0.36
octahedron	QS, mm/s	0.09	0.10	0.15	0.31	0.02
	FWHM, mm/s	0.24	0.27	0.24	0.28	0.24
	S, %	8.3	8.2	6.7	6.0	5.6
	H_{eff}, kOe	407	405	408	399	407
2*b*	IS, mm/s	0.29	0.27	0.29	0.28	0.29
bipyramid	QS, mm/s	2.17	2.12	2.07	2.01	2.11
	FWHM, mm/s	0.28	0.33	0.47	0.31	0.38
	S, %	5.1	4.8	5.2	3.2	6.5

[a] Note. H_{eff} is the hyperfine magnetic field; IS is the isomer shift relative to metallic iron; QS is quadrupole splitting; HW is the half-width of the absorption line; and *S* is the relative area of the MS sextet. Measurement error: H_{eff}, ±5 kOe; IS, QS, and FWHM, ±0.04 mm/s; *S*, ≤6%.

Taking into account the multiplicitiy of structural positions and the same resonant absorption coefficients of iron cations in each position, the ratio of sextet areas (or iron concentrations) relating to the iron positions must be as follows: 12*k*: $4f_1$: $4f_2$: 2*a*: 2*b* = 50:17:17:8:8.

Figure 4 shows plots of the relative areas of sextets (*S*), hyperfine magnetic fields (H_{eff}) and quadrupole splitting (QS) for all positions on the degree of substitution of Co^{2+} and Ti^{4+} for Fe^{3+} ions in sample I. The areas of the MS sextets corresponding to the 12*k* and 2*a* positions of sample I for $x = 0-0.15$ coincide with the theoretical *S* values, 50 and 8%, respectively (Table 1 and Figure 4a). The areas of the $4f_1$ sextets are larger and those of $4f_2$, 2*a* and 2*b* smaller than the theoretical values. Therefore, the Fe^{3+} ions in the BHF structure prefer to occupy tetrahedral $4f_1$ positions in the spinel blocks *S* and *S** (see Figure 4a).

It is known[11] that Ti^{4+} ions, which have a rare gas outer shell, and Fe^{3+} ions, which have a spherically symmetric $3d^5$ electronic shell, are distributed uniformly over the tetra- and octahedral positions of spinel structure. However, Co^{2+} ions prefer octahedral coordination due to d^2sp^3 hybridizations[11,17] and force out Fe^{3+} ions to the tetrahedral positions. Analysis of concentration dependences of relative areas of Mössbauer lines (Figure 4) allows one to suppose that Co^{2+} and Ti^{4+} cations occupy structural positions statistically in the case of their small content ($x \leq 0.2$) and, with increase to $x > 0.2$, partly occupy the positions 12*k*, 2*a*, and 2*b*. The antibate curves $4f_1 - 4f_2$ and 2*a* − 2*b* in the range of $x = 0-0.2$ and decrease in *S* values for the positions 2*a*, 2*b*, and 12*k* in the range of $x = 0.2-0.8$ support this statement.

Figure 5 shows that the increase in the unit cell volume (*V*) of sample I obeys Vegard's law, indicating that substitutional solid solutions are formed. The concentration dependence of unit cell volume correlates well with that of MS parameters: both plots change their slope at $x = 0.2$ (Figures 4 and 5). The decrease in the slope of the $V-x$ plot at $x = 0.2$ (Figure 5) may be due to a decrease in the average cation size because of substitution of Co^{2+} and Ti^{4+} ions for Fe^{3+} ions. In our opinion, Co^{2+} and Ti^{4+} ions are located in the 2*a* and 2*b* positions in the range of $x = 0.2-0.8$. This follows from the concentration dependence of the areas of the MS lines 2*a* and 2*b* (see Figure 4a): the part of Fe^{3+} ions in these positions remains unchanged in the range of $x = 0-0.2$ and decreases in the range of $x = 0.2-0.8$. A substantial increase in the quadrupole splitting of 2*b*-sextet (Table 1, Figure 4c)[4] is also caused by isomorphous substitution in the 2*b* position and distortions of crystal lattice.[18] It is not impossible that Ti^{4+} ions preferably occupy the 2*b* position and that some larger Co^{2+} ions occupy the larger octahedral 2*a* position. Analysis of the effect of the steric factor on the distribution of cations over sites of BHF structure confirms this. For example, the average radius of Fe^{3+} ions in the structure of undoped BHF ($x = 0$) calculated from the areas of MS sextets (see Table 1) is $r(Fe^{3+}) = 0.605$. In calculation we take into account that Fe^{3+} ions are in the high-spin state and have different coordination numbers (CNs): $r(Fe^{3+})_{CN=4,HS} = 0.49$, $r(Fe^{3+})_{CN=5,HS} = 0.58$; $r(Fe^{3+})_{CN=6,HS} = 0.645$.[19] Figure 4 shows that the substitution $2Fe^{3+} \rightarrow Co^{2+} + Ti^{4+}$ occurs in the $4f_2$ and 2*a* positions in the range of $x = 0-0.2$, but this substitution occurs in the 2*a*, 2*b*, and 12*k* positions and results in a decrease of *S* values in the range of $x = 0.2-0.8$. The average radius of $Co^{2+} + Ti^{4+}$ ions in the range of $x = 0-0.2$ is 0.67 ($r(Co^{2+})_{CN=6} = 0.735$, $r(Ti^{4+})_{CN=6} = 0.605$ [19]) and in the range of $x = 0.2-0.8$ is 0.65 (if Ti^{4+} substitutes for Fe^{3+} in the 2*b* position; in this case $r(Ti^{4+})_{CN=5} = 0.57$ [19]) or >0.65 (if Ti^{4+} substitutes for Fe^{3+} in the 2*a* and 2*b* positions). Such distribution of cations on BHF sites agrees with the $V-x$ dependence (see Figure 5). Figure 4b shows that the substitution $2Fe^{3+} \rightarrow Co^{2+} + Ti^{4+}$ in the BHF structure is accompanied by a decrease in H_{eff} values for all positions. H_{eff} decreases due to isomorphous substitutions of iron by other cations.[20] With

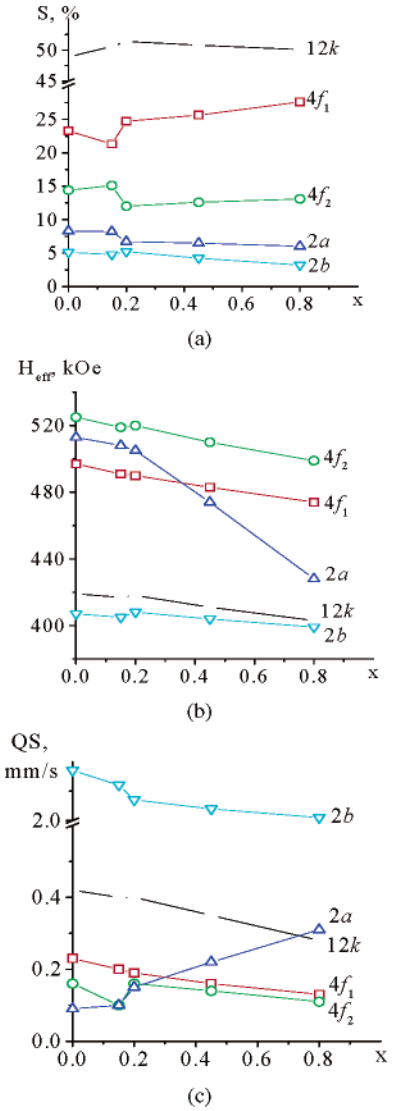

Figure 4. Concentration dependences of relative areas of MS sextets (S), hyperfine magnetic fields (H_{eff}), and quadrupole splitting (QS) for positions 2a, 2b, 4f_1, 4f_2, and 12k of $BaCo_xTi_xFe_{12-2x}O_{19\pm\gamma}$.

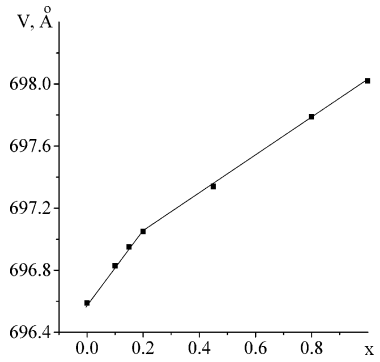

Figure 5. Concentration dependence of the unit cell volume of $BaCo_xTi_xFe_{12-2x}O_{19\pm\gamma}$.

increasing dopant content, the exchange interaction between sublattices decreases, and H_{eff} decreases for all sublattices. Isomorphic shift (IS) does not change with an increase of the degree of isomorphous substitution (Table 1). This indicates that the electronic configuration of Fe^{3+} ions remains unchanged during the substitution $2Fe^{3+} \rightarrow Co^{2+} + Ti^{4+}$. It is noteworthy that H_{eff} decreases sharply on nuclei of ^{57}Fe ions in the range of $x = 0.2-0.8$ and that the quadrupole splitting for Fe^{3+} ions in position 2a increases with increasing x in contrast to its decrease for ions in all other positions (see Figure 4b,c). The dependences of H_{eff} and QS on the x value may be explained by the partial substitution of Ti^{4+} ions for Fe^{3+} ions in position 2a. Therefore, in the range of $x = 0.2-0.8$, Ti^{4+} ions are not only in position 2b (as we conclude from the change of the slope of the $V-x$ plot at $x = 0.2$) but also in position 2a. The presence of small Ti^{4+} ions and large Co^{2+} ions causes local distortion of crystal lattice, and this is accompanied by an increase of QS in position 2a (see Figure 4c). It is known that interaction between nuclei and orbital magnetic moments of 3d electrons make a contribution to the effective magnetic field on nuclei.[21] The partial substitution of Ti^{4+} ($3p^6$) ions for Fe^{3+} ($3d^5$) ions decreases this interaction and the H_{eff} value, which we can see for the position 2a (see Figure 4b).

Thus, complex analysis of concentration dependences of unit cell volume and parameters of Mössbauer spectra allows us to suppose that in the range of $x = 0-0.2$, CO^{2+} and Ti^{4+} ions prefer to substitute for Fe^{3+} ions statistically in the positions 2a and 4f_2. For $x > 0.2$, small Ti^{4+} ions prefer to substitute for Fe^{3+} ions in the positions 2a and 2b, and large Co^{2+} ions prefer to substitute for Fe^{3+} ions in the positions 2a and 12k. Comparison of the areas of MS sextets for all five positions of Fe^{3+} in single-phase cobalt-containing (I) and bismuth-containing (II) BHF (see Table 1) allows us to suppose that Bi^{3+} and Ti^{4+} ions prefer to occupy the positions 2a and 4f_2 and force out Fe^{3+} ions to the position 4f_1.

Magnetic Measurements. Figure 6 shows concentration dependences of the specific saturation magnetization M_s and coercitive force H_c of samples I and II. The specific saturation magnetization of cobalt-containing compositions smoothly increases with increasing dopant content (see Figure 6, curve 1), which agrees with the data of refs 1 and 22, and coercive force almost linearly decreases (Figure 6, curve 3). This is observed in the case of single-domain particles, in which the

TABLE 2: Magnetic Properties of $BaCo_xTi_xFe_{12-2x}O_{19\pm\gamma}$ and $BaBi_xTi_xFe_{12-2x}O_{19\pm\gamma}$ ($T = 1270$ K)[a]

no.	chemical composition	phase composition	B_s, T	B_r, T	B_r/B_s	H_c, kA/m
1	$BaFe_{12}O_{19\pm\gamma}$	BHF	0.30	0.19	0.63	430
2	$BaCo_{0.1}Ti_{0.1}Fe_{11.8}O_{19\pm\gamma}$	BHF	0.34	0.21	0.62	390
3	$BaCo_{0.15}Ti_{0.15}Fe_{11.7}O_{19\pm\gamma}$	BHF	0.345	0.21	0.61	300
4	$BaCo_{0.2}Ti_{0.2}Fe_{11.6}O_{19\pm\gamma}$	BHF	0.37	0.24	0.65	282
5	$BaCo_{0.4}Ti_{0.4}Fe_{11.2}O_{19\pm\gamma}$	BHF	0.38	0.24	0.63	206
6	$BaCo_{0.8}Ti_{0.8}Fe_{10.4}O_{19\pm\gamma}$	BHF	0.39	0.25	0.64	145
7	$BaBi_{0.05}Ti_{0.05}Fe_{11.9}O_{19\pm\gamma}$	BHF	0.34	0.21	0.62	406
8	$BaBi_{0.075}Ti_{0.075}Fe_{11.85}O_{19\pm\gamma}$	BHF	0.35	0.22	0.62	350
9	$BaBi_{0.1}Ti_{0.1}Fe_{11.8}O_{19\pm\gamma}$	BHF	0.35	0.22	0.63	295
10	$BaBi_{0.15}Ti_{0.15}Fe_{11.7}O_{19\pm\gamma}$	BHF	0.36	0.22	0.62	240
11	$BaBi_{0.2}Ti_{0.2}Fe_{11.6}O_{19\pm\gamma}$	BHF + $BiFeO_3$	0.31	0.19	0.61	255

[a] Note. B_s is the maximal magnetic induction; B_r is the residual magnetic induction; and H_c is the coercive force.

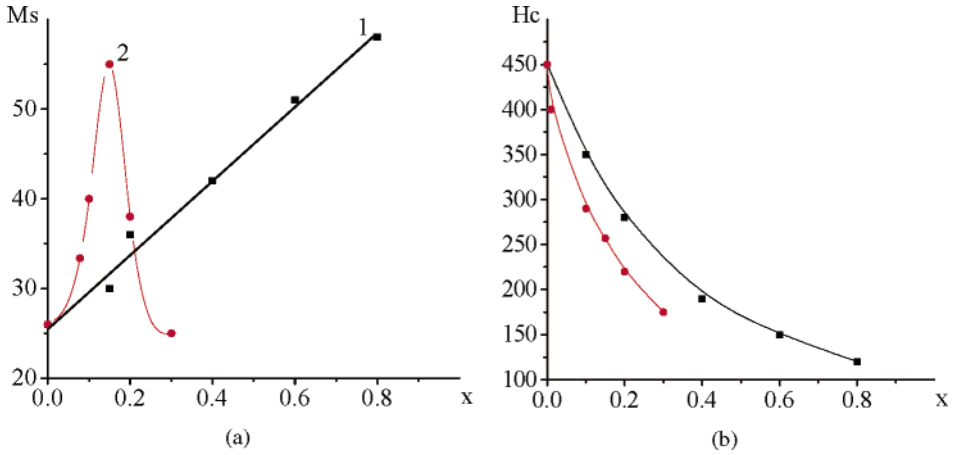

Figure 6. Concentration dependence of saturation magnetization M_s (a) and coercive force H_c (b) for $BaCo_xTi_xFe_{12-2x}O_{19\pm\gamma}$ (1, 3) and $BaBi_xTi_xFe_{12-2x}O_{19\pm\gamma}$ (2, 4).

processes of magnetization and reversal magnetization occur preferably by the mechanism of rotation of magnetization vector. In this case H_c is proportional to the K_1/M_s ratio, where K_1 is the crystalline magnetic anisotropy constant.[1,17] With an increasing amount of Co^{2+} ions, the K_1 value decreases,[17] and this results in a decrease of H_c. The plot of M_s against concentration for $BaBi_xTi_xFe_{12-2x}O_{19\pm\gamma}$ samples has a maximum at $x = 0.15$ (Figure 6, curve 2). This maximum is probably due to the fact that the solubility limit of Bi^{3+} ions is reached at $x = 0.15$ and that they begin to precipitate as a $BiFeO_3$ phase at $x > 0.15$, which is confirmed by X-ray analysis (see Figure 1).

Figure 6 (curves 3, 4) shows that the complex dopant $Bi^{3+} + Ti^{4+}$ is more effective than $Co^{2+} + Ti^{4+}$ in decreasing the coercive force of BHF. Both dopants increase specific saturation magnetization. Such combination of magnetic properties and characteristics of fine ferromagnetic filler based on doped BHF (Table 2) indicates that M-type BHF doped with complex dopant has promise in the production of magnetic data storage media with high recording density.

4. Conclusion

The effect of ($Co^{2+} + Ti^{4+}$) and ($Bi^{3+} + Ti^{4+}$) dopants on the fine structure and magnetic properties of M-type BHF has been studied. It has been shown that in the range of $x = 0-0.2$, Co^{2+} and Ti^{4+} ions prefer to substitute for Fe^{3+} ions statistically in positions 2*a* and $4f_2$ and that, in the range of $x = 0.2-0.8$, Co^{2+} and Ti^{4+} ions substitute for Fe^{3+} ions in positions 2*a*, 2*b*, and 12*k*. In the latter case, Ti^{4+} ions substitute for Fe^{3+} ions in positions 2*a* and 2*b* and Co^{2+} ions substitute for Fe^{3+} ions in positions 2*a* and 12*k* and force out Fe^{3+} ions to positions $4f_1$ and $4f_2$. In single-phase $BaBi_xTi_xFe_{12-2x}O_{19\pm\gamma}$ ($x = 0-0.15$), Bi^{3+} and Ti^{4+} ions prefer to occupy positions 2*a* and $4f_2$ and force out Fe^{3+} ions to position $4f_1$. It has been shown that M-type BHF doped with the complex dopants ($Co^{2+} + Ti^{4+}$) and ($Bi^{3+} + Ti^{4+}$) has promise in the production of magnetic data storage media with high recording density.

References and Notes

(1) Levin, B. E.; Tretyakov Y. D.; Letyuk, L. M. *Physicochemical Background of Preparation, Properties and Application of Ferrites*; Metallurgy: Moscow, 1979.
(2) Zhong, W.; Ding, W.; Zhang, N.; Hong, J. *J. Magn. Magn. Mater.* **1997**, *168*, 196−202.
(3) Zavislyak, I. V.; Kostenko, V. I.; Chamor, T. G.; Chevnyuk, L. V. *Tech. Phys.* **2005**, *75* (4), 128−130.
(4) Kim, C. S.; Lee, S. W.; An, S. Y. *J. Appl. Phys.* **2000**, *87* (9), 6244−6246.
(5) Choi, D. H.; Lee, S. W.; An, S. Y.; Park, S.; Shim, I. *IEEE Trans. Magn.* **2003**, *39* (5), 2884−2886.
(6) An, S. Y.; Shim, I.; Kim, C. S. *J. Appl. Phys.* **2002**, *91* (10), 8465−8467.
(7) Bursik, J.; Simsa, Z.; Stichauer; L.; Tesai, R. *J. Magn. Magn. Mater.* **1997**, *157−158*, 311−312.
(8) Melzer, K.; Suwalski, J.; Lukasiak, M. *Mater. Sci. High Technol.: MASHTEC'90, Proc. Int. Symp.* **1990**, *1*, 275.
(9) Kubo, O.; Nomura, T.; Ido, T. (Kabushiki Kaisha Toshiba (Kawasaki, Japan)) U.S. Pat. 4582623 Apr. 15, 1986.
(10) Ivanova, I. N.; Belyanina, N. V. *Electron. Techn., Iss. "Materials"* **1978**, *4*, 25−29.
(11) Hard-Magnetic Ferrites. Grades and Basic Parameters. SSSR State Standard 24063-80.
(12) Rosler, S.; Wartewig P.; Langbein, H. *Cryst. Res. Technol.* **2003**, *38* (11), 927−934.
(13) Leccabue, F.; Panizzieri, R.; Garsia, S. *J. Mater. Sci.* **1990**, *25* (6), 2765−2770.
(14) Evants, B. J.; Grandjenan F.; Lilot, A. P. *J. Magn. Magn. Mater.* **1987**, *67* (1), 218−224.
(15) Obradors, X.; Solands X.; Collomb, A. *J. Solid State Chem.* **1988**, *72* (2), 218−224.
(16) Thompson, G. K.; Evans, B. J. *J. Magn. Magn. Mater.* **1991**, *95* (2), 1142−1143.
(17) Krupichka, S. *Physic of Ferrites and Allied Magnetic Oxides*; Mir: Moscow, 1976.
(18) Zuravlyov, G. I. *Chemistry and Technology of Ferrites*; Chemistry: Leningrad, 1970.
(19) Shannon, R. D. *Acta Crystallogr.* **1976**, *A32*, 751−767.
(20) Shirane, G.; Cox D. E.; Ruby, S. L. *Rhys. Rev.* **1962**, *125* (4), 1158−1165.
(21) Goldanskii, V. I.; Kriganovskii L. M.; Hrapov, V. V. *Chemical Applications of Mössbauer Spectroscopy*; Mir: Moscow, 1970.
(22) Vasilevskii, Y. A. *Media for Magnetic Recording*; Art: Moscow, 1989.